

Are fossil groups a challenge of the Cold Dark Matter paradigm?

Stefano Zibetti^{1*}, Daniele Pierini², Gabriel W. Pratt²

¹*Max-Planck-Institut für Astronomie, Königstuhl 17, D-69117 Heidelberg, Germany*

²*Max-Planck-Institut für extraterrestrische Physik, Postfach 1312, D-85741 Garching bei München, Germany*

Accepted 2008 October 16. Received 2008 October 15; in original form 2008 July 15

ABSTRACT

We study six groups and clusters of galaxies suggested in the literature to be ‘fossil’ systems (i.e. to have luminous diffuse X-ray emission and a magnitude gap of at least 2 mag-R between the first and the second ranked member within half of the virial radius), each having good quality X-ray data and SDSS spectroscopic or photometric coverage out to the virial radius. The poor cluster AWM 4 is clearly established as a fossil system, and we confirm the fossil nature of four other systems (RX J1331.5+1108, RX J1340.6+4018, RX J1256.0+2556 and RX J1416.4+2315), while the cluster RX J1552.2+2013 is disqualified as fossil system. For all systems we present the luminosity functions within 0.5 and 1 virial radius that are consistent, within the uncertainties, with the universal luminosity function of clusters. For the five *bona fide* fossil systems, having a mass range $2 \times 10^{13} - 3 \times 10^{14} M_{\odot}$, we compute accurate cumulative substructure distribution functions (CSDFs) and compare them with the CSDFs of observed and simulated groups/clusters available in the literature. We demonstrate that the CSDFs of fossil systems are consistent with those of normal observed clusters and do not lack any substructure with respect to simulated galaxy systems in the cosmological Λ CDM framework. In particular, this holds for the archetype fossil group RX J1340.6+4018 as well, contrary to earlier claims.

Key words: galaxies: clusters: general; galaxies: luminosity function, mass function; galaxies: evolution; galaxies: formation; cosmology: observations

1 INTRODUCTION

Early numerical simulations suggested that the most compact galaxy groups could merge to form a single elliptical galaxy (hence a ‘fossil group’) in a few billion years (Barnes 1989). An elliptical galaxy formed by the merger of such a group retains its X-ray emitting halo of hot gas, which is unaffected by merging (Ponman & Bertram 1993). Following this indication, Ponman et al. (1994) discovered the archetype fossil group RX J1340.6+4018.

Vikhlinin et al. (1999) and Jones et al. (2003), on the basis of ROSAT observations, have suggested that fossil groups constitute a considerable population of objects. Their X-ray extent, bolometric X-ray luminosity ($L_{X,\text{bol}} > 10^{42} h_{50}^{-2} \text{ erg s}^{-1}$), dark matter dominated total mass, and mass in the diffuse hot gas component are comparable to those of bright groups and poor clusters of galaxies ($\sim 10^{13} - 10^{14} h_{70}^{-1} M_{\odot}$). The brightest member of a fossil group has an optical luminosity comparable to that of a cluster cD

galaxy (i.e., $M_R < -22.5 + 5 \log h_{50}$) and dominates the galaxy luminosity function of the system. The observational definition of a fossil system lies in the detection of extended, very luminous X-ray emission from the hot gas of the intracluster medium (ICM), and in the existence of an R-band magnitude gap $\Delta m_{12} > 2$ between the brightest and second brightest members within $0.5 R_{\text{vir}}$ (Jones et al. 2000).

As noted by Vikhlinin et al. (1999), fossil groups may represent the ultimate examples of hydrostatic equilibrium in virialised systems, since they must have been undisturbed for a very long time if they are the result of galaxy merging within a group. High-resolution hydrodynamical cosmological simulations in the Λ CDM framework have shown that fossil groups have already assembled half of their final DM mass at redshifts $z \geq 1$, and subsequently they typically grow by minor mergers only, whereas non-fossil systems of similar masses on average form later (D’Onghia et al. 2005). The early assembly of fossil groups leaves sufficient time for objects with luminosities close to the characteristic luminosity (i.e., $L \sim L^*$) to merge into the central galaxy by dynamical friction, producing the magnitude

* E-mail: zibetti@mpia.de

gap which defines a fossil system. In addition, the simulated fossil groups were found to be over-luminous in X-rays relative to non-fossil groups of the same optical luminosity, in qualitative agreement with observations (cf. Vikhlinin et al. 1999; Jones et al. 2000). In a recent paper, von Benda-Beckmann et al. (2008) showed that many galaxy groups may undergo a fossil phase in their lives but may not necessarily stay fossil down to $z = 0$, owing to renewed infall of $L \sim L^*$ galaxies from the large-scale environment. Such infall episodes are statistically more likely for more massive systems, so that the fraction of quasi-fossil systems (i.e. those with a large luminosity gap between the central galaxy and the most luminous satellite) is lower among clusters than among groups (Milosavljević et al. 2006; Yang, Mo, & van den Bosch 2008).

Fossil groups have become a puzzling problem to cosmology since D’Onghia & Lake (2004, DL04) showed that, with respect to state-of-the-art predictions on the frequency of substructures in cold dark matter (CDM) halos (De Lucia et al. 2004), a virialised system like RX J1340.6+4018 lacks galaxies nearly as luminous as the Milky Way. Conversely, the same numerical simulations are able to accurately describe the frequency of substructures in galaxy clusters as massive as Virgo or Coma to well below the circular velocity of a Milky Way-size dark halo (i.e., with $V_{\text{circ}} \leq 220 \text{ km s}^{-1}$). In this respect, fossil groups appeared to exacerbate the so-called ‘small-scale crisis’ of CDM universes (Klypin et al. 1999). In fact, DL04 concluded that the missing substructure problem affects systems up to the scale of groups (typically with $kT_X \leq 1 \text{ keV}$). However, this result has been challenged by Sales et al. (2007), who find that the abundance and luminosity function of simulated fossil systems are in reasonable agreement with the few available observational constraints.

Given the great interest of this cosmological issue, some optical studies have aimed at better characterizing the mass and luminosity function (LF) of already known fossil systems (e.g. Mendes de Oliveira et al. 2006; Cypriano et al. 2006) or identifying new ones (e.g. Santos et al. 2007), although identifying low-mass fossil systems is hampered by the fact that groups are under-represented in existing X-ray catalogs. In spite of the increasing quality of the data and number of candidates, no new cumulative substructure distribution function (CSDF)¹ has so far been produced for a fossil system to compare with that obtained by DL04 for the archetype fossil group RX J1340.6+4018. The determination of the CSDF for fossil systems with a range of masses is the objective of the present study.

In the following, we adopt a Λ CDM cosmological model ($\Omega_m = 0.3$, $\Omega_\Lambda = 0.7$) with $H_0 = 70 \text{ h}_{70}^{-1} \text{ km s}^{-1} \text{ Mpc}^{-1}$. This model is consistent with the main *WMAP5* results (cf. Hinshaw et al. 2008). This work is mainly based on Sloan Digital Sky Survey (York et al. 2000, SDSS) data from the sixth data release (Adelman-McCarthy et al. 2008, DR6, and references therein).

2 THE FOSSIL SAMPLE

In this study we consider five groups and poor clusters of galaxies from the sample of fossil systems originally identified by Ponman et al. (1994) and Jones et al. (2003). In addition we include the poor cluster AWM 4, whose status as fossil system has been suggested by Lin & Mohr (2004) and is established in this work (see Appendix A1). These six systems were selected to have (i) high-quality X-ray observations, either with *Chandra* (Weisskopf et al. 2000) or *XMM-Newton* (Jansen et al. 2001), to allow for a reliable determination of their halo properties (i.e., R_{200} , M_{200} , V_{parent})², and (ii) to be covered by SDSS photometry and, in the case of AWM 4, by SDSS spectroscopy. This enables us to study membership (via spectroscopic redshifts or combining photometric redshifts and statistical foreground/background subtraction) and photometric properties of members across a wide field, out to the virial radius of a system. Such coverage is mandatory to enable us to compare the observed CSDFs with previous determinations and the output of cosmological simulations in the literature, which are normally computed out to the virial radius of a system (i.e., R_{200})³. Table 1 lists coordinates and redshifts of the six systems.

2.1 X-ray data

The X-ray and derived halo properties are reported in Table 2, along with the references to the works from which these data are taken. For all systems (except AWM 4 and RX J1416.4+2315) M_{200} and R_{200} are computed from the X-ray temperatures published by Khosroshahi et al. (2007) using the scaling relations given by Arnaud et al. (2005). We adopt their fits to the $M_{200} - T_X$ and $R_{200} - T_X$ relations of the entire sample to derive our fiducial estimates. In our analysis in Sect. 3 we consider the effect of estimating mass and radius from fits to both the entire sample of Arnaud et al. (2005), which has a slope of 1.71, and from fits to the hot systems alone ($kT > 3.5 \text{ keV}$), which has a slope of 1.49. The resulting masses are reported in Table 2. Our motivation for this choice of relation is based on the recent results of Sun et al. (2008), who derive the mass temperature scaling relation from 1 to 10 keV using high quality *Chandra* data of a large sample of groups and clusters. Their $M - T$ relation normalisation is similar to that of Arnaud et al. (2005), and they find a slope of 1.67, such that group masses would be 18 per cent higher at 1 keV than that derived from the fit to the full sample of Arnaud et al. (2005). In using both Arnaud et al. relations we wish to attempt to bracket the most likely value of the $M - T$ normalisation in this mass range. We note however that Khosroshahi et al. (2007) suggest that fossil groups may fall low on the $M - T$ relation, although Sun et al. (2008) find no evidence for this with a smaller sample of fossil groups. The extent of the offset found by Khosroshahi et al. appears

¹ The cumulative substructure distribution function gives the number of sub-halos with circular velocity V_{circ} larger than a given fraction of the circular velocity of the parent halo V_{parent} .

² R_{200} is the radius within which the average density of the system is 200 times the critical density of the Universe. M_{200} is the mass within R_{200} .

³ Throughout the paper we use R_{200} as a proxy for the virial radius R_{vir} .

to be mass dependent and is negligible at higher group temperatures ($kT \gtrsim 2$ keV), although it could be up to a factor of 2-3 for the very lowest temperature systems. Deeper X-ray observations of fossil groups have been obtained to help resolve this issue, and will be the subject of a forthcoming paper.

As we show in Sect. 3, the CSDFs we derive are relatively insensitive to the exact choice of X-ray scaling relation and our conclusions are robust in case fossil groups should indeed fall low on the $M - T$ relation.

For AWM 4 and RX J1416.4+2315, estimates of M_{200} and R_{200} are taken from Gastaldello et al. (2007) and Khosroshahi et al. (2006), respectively, who fitted NFW profiles (Navarro et al. 1997) to the observed mass density profiles of these two systems. It is worth noting that there is a very good agreement between the estimates given in the two papers referred above and those derived from the scaling relations of Arnaud et al. (2005). From Table 2 one can clearly see that our sample spans a broad range in mass and X-ray temperature, in the regime of groups and poor clusters.

Once M_{200} and R_{200} are obtained, the circular velocity of the parent halo of each system is computed :

$$V_{\text{parent}} = \sqrt{\frac{GM_{200}}{R_{200}}} \quad (1)$$

2.2 Optical data

With the exception of AWM 4, the nearest cluster at $z = 0.0317$, the analysis of all systems relies on SDSS photometric data only (including photometric redshifts). Although for some of them spectroscopic redshifts are available through the SDSS or other published catalogs, the lack of completeness or insufficient depth prevents us from using them. The SDSS spectroscopic data, in particular, are limited to 17.77 mag (r band, see Strauss et al. 2002); this translates into absolute magnitude limits ranging from -20 (for RX J1331.5+1108 at $z = 0.081$) to -22.5 (for RX J1256.0+2556 at $z = 0.23$), thus making the faint end of the luminosity function inaccessible to our analysis. In contrast, assuming a conservative limit of 20.5 r -mag, the SDSS photometry allows us to probe down to roughly one magnitude fainter than L^* for all systems. Although one could in principle combine the complete information derived from photometric data alone with the spectroscopic memberships for the brightest galaxies or in the regions covered by other surveys, combining different selection functions is an unnecessary complication. In particular, we have checked that for all bright galaxies ($r < 17.77$ mag) with available spectroscopy the spectroscopic membership coincides with the purely photometric one.

In Appendix A we comment further on issues specific to individual systems and on their status of fossil. In summary, AWM 4 is established as fossil; RX J1331.5+1108, RX J1340.6+4018 and RX J1416.4+2315 are confirmed fossil systems; observational uncertainties do not allow us to establish RX J1256.0+2556 as a fossil with very high confidence, but we will consider it as a fossil in the following; lastly, RX J1552.2+2013 does not match the magnitude gap requirement and is disqualified as a fossil system.

Table 1. The sample

Denomination	RA (J2000.0)	Dec (J2000.0)	z
AWM 4	16:04:57.0	+23:55:14	0.0317
RX J1256.0+2556	12:56:03.4	+25:56:48	0.2320
RX J1331.5+1108	13:31:30.2	+11:08:04	0.0810
RX J1340.6+4018	13:40:33.4	+40:17:48	0.1710
RX J1416.4+2315	14:16:26.9	+23:15:32	0.1370
RX J1552.2+2013	15:52:12.5	+20:13:32	0.1350

3 THE CUMULATIVE SUBSTRUCTURE DISTRIBUTION FUNCTION: METHOD

In this section we describe how the cumulative substructure distribution function is computed for the systems in our sample. As mentioned in Sect. 1, the CSDF of a galaxy system, $N(> x \equiv V_{\text{circ}}/V_{\text{parent}})$, is defined as the number of members (i.e., substructures of the parent DM halo), other than the brightest member, which are satellites and have circular velocities V_{circ} larger than xV_{parent} . Here V_{parent} is the circular velocity of the parent system considered as a whole (defined in Eq. 1) and $x < 1$. Theoretically, each galaxy in a group/cluster is associated with a DM sub-halo of a given mass M_{sub} and radius R_{sub} such that the circular velocity is simply defined as $V_{\text{circ}} = \sqrt{GM_{\text{sub}}/R_{\text{sub}}}$. Observationally this information is only accessible for few well studied galaxies. For the galaxies in our systems circular velocities must be derived from basic observables (luminosity, central velocity dispersion) by means of scaling relations, as we describe in Sect. 3.1.

The second essential ingredient for computing the CSDF is the method to count galaxies up to a given circular velocity, either by means of a complete cluster membership selection based on spectroscopic redshifts, or by means of a robust statistical subtraction of the galaxy foreground/background from the counts in the cluster/group region. This is discussed in Sect. 3.2.

3.1 Inferring V_{circ}

The structure and luminosity of galaxies are known to be linked to their kinematics via scaling relations. For late-type (spiral) galaxies the Tully-Fisher (TF) relation (Tully & Fisher 1977) links luminosity and (maximum or asymptotic) circular velocity in the disk, which we assume to coincide with V_{circ} ⁴. For early-type (elliptical) galaxies the central velocity dispersion σ_0 can be inferred either from the luminosity using the Faber-Jackson (FJ) relation (Faber & Jackson 1976) or, when more information about the surface brightness distribution is available, via the fundamental plane (FP) relation that connects half light radius, effective surface brightness, and central velocity dispersion σ_0 . Once σ_0 is known, the circular velocity can then be inferred. In doing so, one can either assume isothermal dynamics, in which case $V_{\text{circ}} \approx \sqrt{2}\sigma_0$, or adopt empirical scaling relations between the two quantities based on very

⁴ This is an approximation that may lead to a systematic overestimate of the true V_{circ} at the sub-halo virial radius by some 10 per cent (see Salucci et al. 2007).

Table 2. X-ray and halo properties of the sample systems

Denomination	kT_X [keV]	L_X^a [10^{42} erg s $^{-1}$]	M_{200} [10^{13} M $_{\odot}$]	R_{200} [Mpc]	R_{200} [arcmin]	V_{parent} [km s $^{-1}$]	Ref. ^b
			‘hot’	‘hot’	‘hot’	‘hot’	
AWM 4	2.48 ± 0.06	39.3^c	13.75 ± 1.46	...	1.054 ± 0.038	...	G07
RX J1256.0+2556	2.63 ± 1.13	50.0	$15.75^{+13.38}_{-9.75}$	19.63	$1.034^{+0.234}_{-0.283}$	$4.66^{+1.07}_{-1.28}$	K07
RX J1331.5+1108	0.81 ± 0.04	2.1	2.25 ± 0.19	3.67	0.571 ± 0.016	6.23 ± 0.17	K07
RX J1340.6+4018	1.16 ± 0.08	5.2	$3.98^{+0.48}_{-0.46}$	5.99	0.670 ± 0.026	3.83 ± 0.14	K07
RX J1416.4+2315	4.00 ± 0.62	170.0	31.00 ± 10	...	1.220 ± 0.060	8.39 ± 0.41	K06
RX J1552.2+2013	2.85 ± 0.90	60.0	$19.03^{+11.48}_{-9.12}$	23.28	$1.139^{+0.193}_{-0.222}$	$7.93^{+1.34}_{-1.55}$	K07

^a Bolometric, within R_{200} , unless specified otherwise.

^b G07=Gastaldello et al. (2007), K07=Khosroshahi et al. (2007), K06=Khosroshahi et al. (2006)

^c Within 455 kpc, (0.1–100 keV)

deep observations of extended rotation curves in early-type galaxies (e.g. Pizzella et al. 2005; Ferrarese 2002). In the following analysis we adopt the relation given by Pizzella et al. (2005), viz.,

$$V_{circ} = (1.32 \pm 0.09)\sigma_0 + (46 \pm 14) \quad [\text{km s}^{-1}] \quad (2)$$

as it includes a comprehensive sample of both low and high surface brightness galaxies over the range between ~ 50 and 350 km s^{-1} , and is therefore best suited for an heterogeneous sample like ours. In fact Equation 2 applies to every galaxy, irrespective of its morphological type, provided that the central velocity dispersion is measured.

We note that the analysis presented in this work relies on the reasonable assumption that scaling relations hold everywhere and phenomena like the tidal truncation of sub-halos do not modify them significantly.

In practice, we are faced with very different kinds of data, requiring a diversity of approaches, as we now describe.

3.1.1 V_{circ} in AWM 4

Most of the galaxies in AWM 4 have a measured velocity dispersion from SDSS spectra. For these galaxies we first correct the measured value for the standard aperture corresponding to the effective radius $r_e/8$, using the recipe given by Jørgensen et al. (1995). Then we apply the scaling relation of Pizzella et al. (2005) to infer V_{circ} .

In cases where the velocity dispersion is not available, the relatively small distance to this cluster allows a reliable estimate of the structural parameters of the galaxies to be achieved. Hence we proceed as follows.

(i) First we select early-type galaxies based on the concentration index $C_i \equiv R_{90 \text{ Petro},i}/R_{50 \text{ Petro},i} > 2.5$ as given by the SDSS in i -band (as in Bernardi et al. 2003a). For these galaxies σ_0 is derived from the r -band FP relation of Bernardi et al. (2003c), after applying k and cosmological dimming $[(z+1)^4]$ corrections to the effective surface brightness. Thereafter σ_0 is converted into V_{circ} using the Pizzella et al. (2005) relation as detailed above.

(ii) Bright galaxies (rest-frame $M_i < -19$ mag) with $C_i \leq 2.5$ are considered *bona fide* disc-dominated galaxies and their V_{circ} is computed via the TF relation. In order to minimise systematic errors, our best estimate of V_{circ} is given by the mean of the TF estimate of Pizagno et al. (2007, using i -band Petrosian magnitudes) and of Tully et al. (1998, us-

ing i -band ‘total’ composite model magnitudes converted to I_C). In both cases magnitudes are k -corrected and corrected for the inclination-dependent internal extinction using the recipe of Tully et al. (1998). i and I_C bands are explicitly chosen to minimise the amount and uncertainty of this correction (cf. e.g. Pierini 1999; Pierini et al. 2003).

(iii) Finally, for galaxies fainter than $M_i = -19$ mag and with $C_i \leq 2.5$, the concentration index is not indicative of the dynamical state (e.g. dwarf elliptical galaxies can be ‘hot’ systems yet have low concentration). In this case our best guess V_{circ} is given by the mean of the estimate from the FP – as in case (i) – and from the TF – as in case (ii).

Statistical errors are computed by summing uncertainties on the measured quantities propagated to V_{circ} and the typical r.m.s. scatter around the scaling relations, in quadrature. In particular, we adopt a scatter of 15 km s^{-1} for V_{circ} in the Pizzella et al. (2005) relation, 10% r.m.s. for σ_0 from the FP, and 15% for V_{circ} about the TF relation (Pizagno et al. 2007). The effect of random errors on the CSDF are quantified by means of Monte Carlo simulations (see Sect. 4.2).

Systematic errors may have even greater impact on our conclusions about the CSDFs as they can shift or expand/shrink the real distributions. We consider systematic uncertainties for all adopted scaling relations. In the FP and Pizzella et al. (2005) relation we use the uncertainties on the fitting parameters given in the reference papers. In particular, for the Pizzella et al. (2005) relation we account for the covariance between the two fitted coefficients by re-writing the fitting function referred to the mean abscissa of the points and considering only the error on the slope. The covariance terms between the FP parameters can then be safely neglected as Fig. 2 of Zibetti et al. (2002) illustrates. For the TF estimates we adopt half of the range spanned by the two relations of Pizagno et al. (2007) and Tully et al. (1998) as a systematic uncertainty.

The set of all possible systematics and their permutations gives us useful upper and lower limits for the computed CSDFs, as we will show in Fig. 3.

3.1.2 V_{circ} for RX groups/clusters

For the five RX systems we rely on photometric data alone to compute V_{circ} for the reasons outlined in Sect. 2. In addition, their higher redshift relative to AWM 4 makes the use

of structural parameters much more uncertain. Moreover, uncertainties on membership determined through statistical methods (see Sect. 3.2) will completely dominate over the uncertainties brought in by the scaling relations. Therefore we simplify the procedure described above.

For the RX systems we determine V_{circ} (i) either using the TF relation of Pizagno et al. (2007) for the most accurate r band or (ii) by converting σ_0 , inferred from the r -band magnitude via the FJ relation of Bernardi et al. (2003b), into V_{circ} using the Pizzella et al. (2005) relation. The choice between the two is dictated by the colour of the galaxy, according to the well known colour bimodality (e.g. Baldry et al. 2004). For each cluster/group we look at the $g-i$ colour distribution of galaxies with a photometric redshift close to the redshift of the system, and determine *by eye* the cut between *blue* and *red* galaxies. The values of V_{circ} of the former are determined via the TF relation, while for the latter we use the combination of FJ and Pizzella et al. (2005) relations.

All magnitudes we use for the scaling relations are taken from SDSS-DR6 and are corrected for foreground Galactic extinction, redshift (k -corrections as given by Csabai et al. 2003) and, for red galaxies only, passive stellar evolution, according to the output of the code of Bruzual & Charlot (2003). We have checked that our results are largely insensitive to the particular choice of colour cut or, alternatively, to a cut in spectral type, as derived from the photometric redshift algorithm (see Csabai et al. 2003, for details).

3.2 Membership and statistical foreground/background subtraction methods

With the exception of AWM4, for which cluster membership is assigned to individual galaxies via spectroscopic redshifts (see Sect. A1), member galaxy counts are based on photometric redshifts from the SDSS-DR6 (Csabai et al. 2003) and are obtained after application of statistical foreground/background subtraction methods.

For each system, we define a circle corresponding to the projected R_{200} , centered at the coordinates of the peak of the X-ray emission, and 1 000 control fields of the same circular aperture, randomly distributed inside an annulus with inner radius $2R_{200}$ and outer radius 4 degrees. The inner radius is chosen to avoid the cluster region, while the outer radius allows us to avoid control field overlapping. We assume each galaxy lies at the redshift of the system in question, and the corresponding property X (e.g. absolute magnitude, velocity etc.) is computed. Galaxy number distributions for the property X are computed in the cluster region ($D_0(X)$) and in the control fields ($D_i(X)|_{\{i=1,1000\}}$). The “true” distribution for the cluster is then given by $D_{\text{cluster}}(X) = D_0(X) - \overline{D(X)}$, where $\overline{D(X)}$ is the median value of $D_i(X)$ over i for any given value of X .⁵ The confidence range for $D_{\text{cluster}}(X)$ is

given by the distributions obtained by replacing the median value of $D_i(X)$ with the 16th and 84th percentile values.

Although in principle this method does not require any pre-selection of galaxies, the background contamination is exceedingly high with respect to the net signal contributed by the cluster, so that a careful pre-selection is mandatory. To this end we use photometric redshift estimates and shape classifications provided by the SDSS for every source. Considering the distances to our systems and the limiting magnitude of 20.5 r -mag (Petrosian, corrected for foreground Galactic extinction), all cluster/group galaxies should be safely resolved even in the worst case of a PSF FWHM equal to $1.5''$. Therefore we initially select only sources classified as extended (“GALAXIES”).

We then apply a cut in photometric redshift to exclude the largest possible number of contaminants in the foreground and background, but avoiding exclusion of system members. Unfortunately photometric redshifts are typically affected by significant uncertainties, from 0.03 r.m.s. at 16 r -mag to 0.08 at 20.5 r -mag (Csabai et al. 2003). Therefore the selected ranges $z_{\text{sys}} \pm \Delta z$ need to be quite broad. We optimise the result by adapting the cut widths Δz to linearly scale as a function of apparent magnitude, such that $\Delta z(m_r = 14.5) = 0.05$ and $\Delta z(m_r = 20.5) = 0.1$.

This pre-selection in photometric redshift and stellar-index index allows us to attain a satisfactory signal-to-noise (S/N), while leaving us with a clean and unbiased selection. This is confirmed by the stability of our distributions when we adopt less restrictive cuts (at the cost of a degradation in S/N however). Moreover, as already mentioned in Sec. 2.2, the memberships of the brightest galaxies based on this photometric method coincide with those resulting from spectroscopic redshifts, whenever these are available. As a key test for our method, we next discuss the luminosity functions for all of our systems.

4 RESULTS

4.1 The luminosity function of fossil systems

Figure 1 shows the luminosity function (LF) of the six galaxy systems. The objects are plotted from left to right and from top to bottom in order of ascending circular velocity V_{parent} . We examine the LF in two apertures, namely within R_{200} (blue filled histograms and magenta lines) and $0.5R_{200}$ (black hatched histograms and black lines). For all systems but AWM4 error bars show the confidence intervals derived from control field statistics.

The solid curves represent the universal LF of Popesso et al. (2005), normalised to the total number of galaxies down to 20 r -mag (apparent). We stress that no other parameter is tuned in order to improve the match between these curves and the measured histogram. Errors are too large to claim any agreement or disagreement with the universal LF for the least massive groups, because of the small number statistics and the weak contrast against the background. For the three most massive systems, however,

⁵ The distribution computed in this way actually measures the *excess* of counts in the cluster vs. the field. To obtain the true cluster counts, we correct the field counts by subtracting the contribution of the physical space that would be occupied by the cluster. Such a correction is well below the per cent level in all cases.

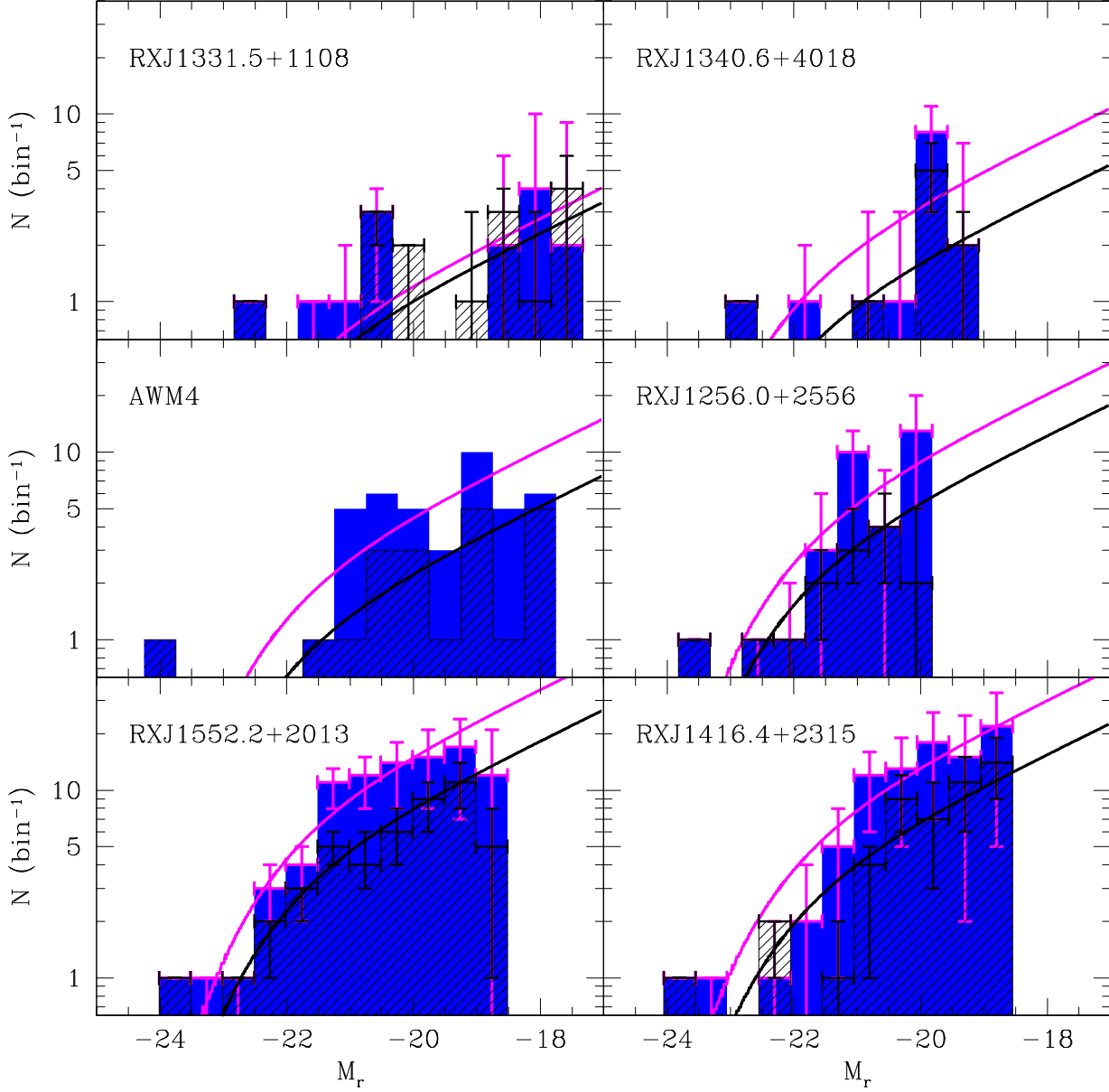


Figure 1. The luminosity function of the six galaxy systems, ordered by ascending circular velocity from left to right and top to bottom. Counts are per bin of magnitude (0.5 mag width). Filled blue histograms and magenta symbols represent the entire area within R_{200} , hatched histograms and black symbols represent the area within $0.5R_{200}$. Error bars are derived via statistical methods (see text for details). The curves represent the analytical LF of Popesso et al. (2005a), normalised to the total number of galaxies down to 20 r -mag (apparent), with no other adjustable parameter.

the plots show an almost perfect agreement within the error bars⁶.

The normalization N of the LF⁷ scales, as expected, with cluster mass or, equivalently, with X-ray temperature,

⁶ Note that the brightest galaxy is not considered as part of the regular luminosity function.

⁷ N is the number of galaxies per 0.5 mag at $M_r = -18.0$.

as we show in Fig. 2. The orthogonal fit to the data points (solid line) gives $N \propto L_X^{1.79 \pm 0.33}$, where the error on the exponent is formally derived under the hypothesis of gaussian errors. If the assumption is made that the total optical luminosity of the cluster (r -band), $L_{\text{opt},r}$, scales proportionally to N , we can compare this result with the finding of Popesso et al. (2004): $L_{\text{opt},r} \propto L_X^{1.1}$ (dashed line in Fig. 2). Formally our relation is significantly (at more than 2 sigmas) steeper than the one found by Popesso et al. (2004),

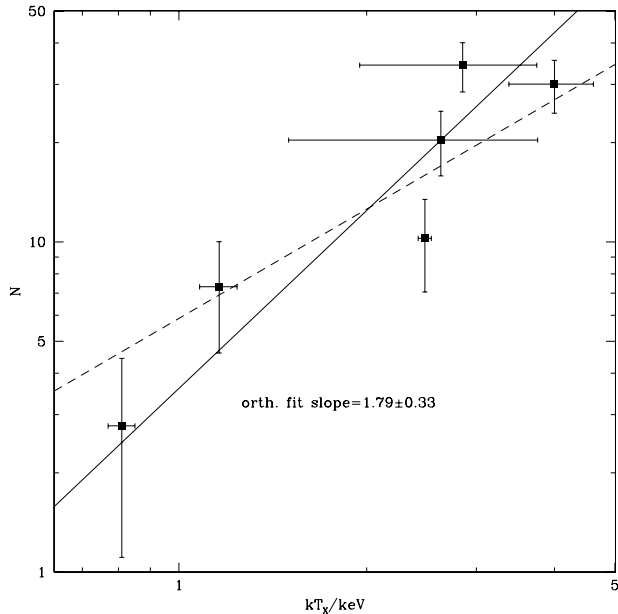


Figure 2. The “galaxy richness” of the systems N versus the X-ray temperature. The solid line is the orthogonal least squares fit to the points, assuming poisson errors on the number counts. The slope is reported in the panels. The dashed line shows the slope of 1.1 for the analogous relation observed by Popesso et al. (2004).

but consistent with the $3/2$ slope expected for self-similar systems. However, our small number statistics and possible systematics hidden behind the assumption $L_{\text{opt},r} \propto N$ prevent us from drawing any quantitative conclusion.

The LFs within $0.5R_{200}$ also confirm the magnitude gaps typical of fossil systems (see Appendix A). This is particularly remarkable as it shows that the photometric redshift pre-selection works very well in the bright regime, and provides very high completeness and low contamination.

Finally we note that the LF (inside $0.5R_{200}$) for RX J1416.4+2315 and RX J1552.2+2013 are in very good *quantitative* agreement with those determined by Cypriano et al. (2006) and Mendes de Oliveira et al. (2006), respectively, based on spectroscopic membership determination. A detailed comparison indicates that the drop of number counts that we observe in RX J1552.2+2013 at $M_r > -19$ mag is fully consistent with the observations of Mendes de Oliveira et al. (2006), and therefore is most likely real.

In light of the above we conclude that our statistical method of membership estimation is sufficiently robust and accurate to study the LF, and hence is applicable also to study of the CSDF.

4.2 Substructure Distribution Functions

Cumulative substructure distribution functions are constructed following different methods for AWM 4 and the five RX systems. In the case of AWM 4 all spectroscopic members are used directly to build the CSDF from their estimated $V_{\text{circ}}/V_{\text{parent}}$. In the case of RX systems, the method

described in Sect. 3.2 is adopted with the property X replaced by $V_{\text{circ}}/V_{\text{parent}}$. The CSDFs obtained in this way, assuming the values of V_{parent} given in Table 2, are shown as thick blue lines in Fig. 3.

The limiting magnitudes that define the completeness of our sample translate into a very complicated completeness function for $V_{\text{circ}}/V_{\text{parent}}$ because of the different scaling relations adopted. By inverting each scaling relation we calculate the set of V_{circ} corresponding to the limiting magnitudes of our samples. The maximum among these values is then our completeness limit for the CSDF. The CSDFs of the RX systems are cut at this limit in Fig. 3. For AWM 4 the entire CSDF is shown, and the completeness limit is marked with a vertical dashed line.

Figure 3 also shows statistical and systematic uncertainties. Concerning AWM 4, the V_{circ} of each galaxy has an associated error. To quantify the effect of these uncertainties on the CSDF we run 10 000 Monte Carlo simulations offsetting each V_{circ} by a random Δv drawn from a Gaussian distribution with the same width as the associated uncertainty. For each realization the CSDF is computed. The confidence range is determined from the 16th–84th percentile range of $V_{\text{circ}}/V_{\text{parent}}$ at each step of the CSDF, and is shown as the cyan shaded area in Fig. 3. This randomisation procedure is undertaken assuming the standard scaling relations. If we now let the parameters of the scaling relations vary within their uncertainties, we obtain the orange and the magenta hatched regions as extreme cases. On the other hand, the X-ray data appear to be good enough to determine R_{200} and V_{parent} with an accuracy of better than 10 per cent. This implies that galaxy counts would change only slightly, and the CSDF could shift horizontally by 10 per cent at most, which is comparable to or less than the effect of other systematic uncertainties.

For the five RX systems, we consider only uncertainties due to statistical foreground/background subtraction and to the determination of the properties of the parent system. The cyan shaded areas in Fig. 3 show the 16th–84th percentile range of variation due to the statistical uncertainties of background counts. The red thick lines represent the CSDFs that we obtain by adopting the X-ray scaling relations determined from systems with $kT > 3.5$ keV instead of the full range (i.e., the parent system parameters derived from the ‘hot’ scaling relations, see Sect. 2). The range of variation due to each uncertainty is of the same magnitude at the lower end of the mass range; at higher masses, uncertainties due to statistical foreground/background subtraction dominate.

We note that the observed $M - T_X$ relations exhibit normalizations which are lower than those produced from simulations by a factor of ~ 10 per cent, perhaps due to a neglect of non-thermal pressure support (Arnaud et al. 2005; Vikhlinin et al. 2006; Nagai et al. 2007). Such a systematic effect would lead us to underestimate both R_{200} and V_{parent} in the calculation of the CSDFs. This would tend to shift all CSDFs slightly down and to the right in Fig. 3. On the other hand, if fossil groups had lower masses for a given T_X as claimed by Khosroshahi et al. (2007), their CSDFs would shift to the right, in the sense of more abundant substructure. This should mainly affect groups with $kT_X \lesssim 2$ keV, i.e. only RX J1331.5+1108 and RX J1340.5+4017 in our sample. It is worth noting, however, that these two

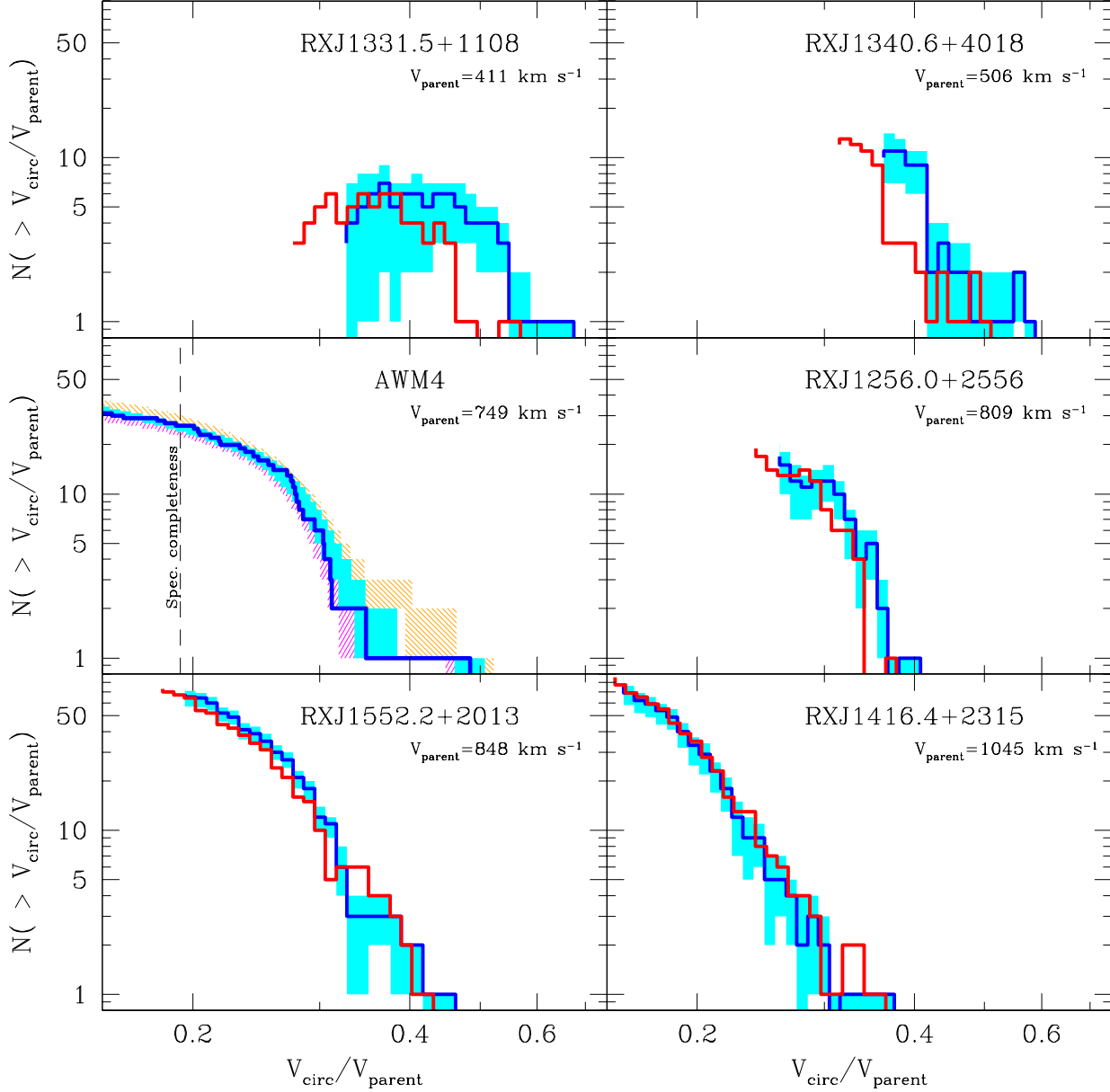


Figure 3. The cumulative substructure distribution functions of the six galaxy systems, ordered by ascending circular velocity from left to right and top to bottom. The blue lines are our fiducial CSDF determinations. Cyan areas display statistical uncertainties. Red lines and hatched areas (for AWM 4) show the effect of systematic uncertainties, as described in the text.

groups are those that lie closer to the $M - T$ relation of normal groups (see Khosroshahi et al. 2007, their Figure 8). By comparing R_δ and M_δ at overdensity $\delta = 500$ as given by Khosroshahi et al. (2007) and as estimated from our fiducial scaling relations (Arnaud et al. 2005), we conclude that the CSDFs of RXJ1331.5+1108 and RXJ1340.5+4017 could further shift to higher $V_{\text{circ}}/V_{\text{parent}}$ by 25 and 17 per cent respectively. Errors in the X-ray temperature itself propagate quite weakly on the CSDF. The effect of under(over)-estimating T_X is to under(over)-estimate both R_{200} and

V_{parent} , with the result of decreasing (increasing) the galaxy counts but simultaneously shifting the distribution to the right (left).

5 DISCUSSION

Figure 3 shows an interesting feature: the CSDFs shift to lower $V_{\text{circ}}/V_{\text{parent}}$ by almost a factor of two as the mass of the system increases. Noticeably this is in agreement with the statistical behaviour of $V_{\text{circ},2\text{nd}}/V_{\text{parent}}$ for the second

brightest member of SDSS groups/clusters as a function of mass as presented by Yang, Mo, & van den Bosch (2008). From their Figures 6 and 7 we compute that $V_{\text{circ,2nd}}/V_{\text{parent}}$ decreases by ≈ 0.24 dex when M_{200} increases from 2×10^{13} to $3 \times 10^{14} M_{\odot}$, as in our sample. This decrease nicely matches the shift observed in Fig. 3 and does not point to any anomalous behaviour of fossil with respect to non-fossil systems of the same mass.

As a test, following Sales et al. (2007) we compute the magnitude gap between the first and the tenth ranked member ΔM_{10} of AWM 4, using the spectroscopic membership determinations. With a central galaxy luminosity $L = 2.34 \times 10^{11} L_{\odot}$ and $\Delta M_{10} = 3.29$ mag, AWM 4 falls in the region covered by the simulations of isolated bright galaxies by Sales et al. (2007, their Figure 3). Once more, this suggests that fossil systems are not anomalous when compared to current Λ CDM simulations.

To better prove this, we compare the CDFs of the five *bona fide* fossil systems with those of observed nearby clusters/groups and of simulated systems in the Λ CDM framework. In particular we refer to the results presented in Desai et al. (2004, their Figure 5). These authors have measured CSDFs for 34 clusters/groups identified in the SDSS, with velocity dispersions ranging from 250 to 1000 km s^{-1} . Desai et al. (2004) also consider 15 simulated groups/clusters in approximately the same velocity dispersion range and measured the corresponding CSDFs. Figure 4 reproduces their observed (*left panel*) and simulated CSDFs (*right panel*) as hatched areas, overlaid onto the CSDFs of our five fossil systems (grey-shaded areas, displaying the range of statistical uncertainties, equivalent to the cyan area in Fig. 3; the thick black lines are the CSDF of AWM 4).

The CSDFs of all fossil systems fall in the range of measured CSDFs for SDSS clusters. In comparison to simulations the CSDFs of our fossil systems are generally in good agreement, although an excess of substructure is observed at high $V_{\text{circ}}/V_{\text{parent}}$. This discrepancy is seen also between the real and the simulated clusters by Desai et al. (2004). As these authors show (their Section 6.4), it most likely results from not properly taking the effects of baryons into account in simulations. What is most interesting to note here, however, is that none of the fossil systems appears to be lacking significant amount of substructure, this result being robust against systematic effects induced by different choices of scaling relations.

In particular, we are unable to reproduce the results of DL04 concerning RX 1340.6+4018: although with large uncertainties, the archetype fossil group does not show any evidence for missing substructure. We note that the entire CSDF of DL04 (their Fig. 1) is shifted to a factor of two lower velocities with respect to ours. This might result from a different choice of scaling relations, although (as we show for AWM 4) choices within a reasonable range of parameters cannot change the results by such a large amount. Moreover our photometric dataset allows us to apply scaling laws in a very accurate and galaxy-type specific way, as detailed in Sect. 3.1.2. In contrast to DL04 we also take advantage of a much better and more complete sample selection, based on complete photometric coverage over the entire virialised region of the group, and perform robust statistical foreground/background subtraction. Finally, we have thoroughly investigated all possible sources of uncer-

tainty which could propagate into our determination of the CSDFs of these systems, finding them all to be relatively small.

In conclusion, the present analysis rules out lack of substructure in fossil clusters ($M_{200} \gtrsim 10^{14} M_{\odot}$), where our two photometrically derived CSDFs are robust and consistent with the CSDF of AWM 4 based on spectroscopy. The same appears to hold for lower mass fossil systems, although with non-negligible uncertainties. Spectroscopic determinations of CSDFs for fossil groups ($M_{200} \approx 10^{13} - 10^{14} M_{\odot}$) would greatly help to reach a firm conclusion in this mass range.

6 CONCLUSIONS

We have studied six galaxy groups and clusters suggested in the literature to be fossil systems, and having high quality X-ray and SDSS spectroscopic or photometric information. Among them, we have established AWM 4 as fossil system. We confirm three other systems (RX J1331.5+1108, RX J1340.6+4018 and RX J1416.4+2315) to be fossil. RX J1256.0+2556 has characteristics very close to a genuine fossil system, although observational errors are still too large for a robust classification as fossil. Finally we demonstrate that RX J1552.2+2013 does not match the magnitude gap requirement to qualify as a fossil.

For each system we have computed the luminosity functions within 0.5 and 1 virial radius. Although with uncertainties, that are remarkably large for the least massive systems, they are consistent with the universal luminosity function of clusters derived by Popesso et al. (2004).

We have derived detailed cumulative substructure distribution functions (CSDFs) for the six galaxy groups and clusters. Our motivation was to produce CSDFs for systems with a range of masses in the group and poor cluster regime, for comparison with the original CSDF derived for the archetype fossil system RX J1340.6+4018 by D’Onghia & Lake (2004, DL04). In fact, these authors claimed a lack of substructure for RX J1340.6+4018, suggesting that the so-called ‘small-scale crisis’ of Milky-Way-size haloes (Klypin et al. 1999) exists up to the scale of X-ray bright groups. In addition we wanted to compare the CSDFs of our fossil systems with results from normal groups and clusters identified in the SDSS (Desai et al. 2004), and in cosmological simulations (Desai et al. 2004; Sales et al. 2007).

Our conclusions are as follows:

- The CSDF of AWM 4, based on spectroscopic data, is completely consistent both with Desai et al. (2004)’s data and with simulations. AWM 4 also matches the simulations by Sales et al. (2007) of isolated bright galaxies in terms of central galaxy luminosity vs. magnitude gap between the first and the tenth ranked member.
- The photometrically derived CSDFs of the other four *bona fide* fossil systems are all completely consistent with the CSDF envelope derived from observed normal groups and clusters (Desai et al. 2004). With respect to numerically simulated systems in Desai et al. (2004) none of our fossil systems appears to lack any substructure.

We therefore conclude that no evidence can be provided that the ‘small-scale crisis’ is occurring on the scale of fos-

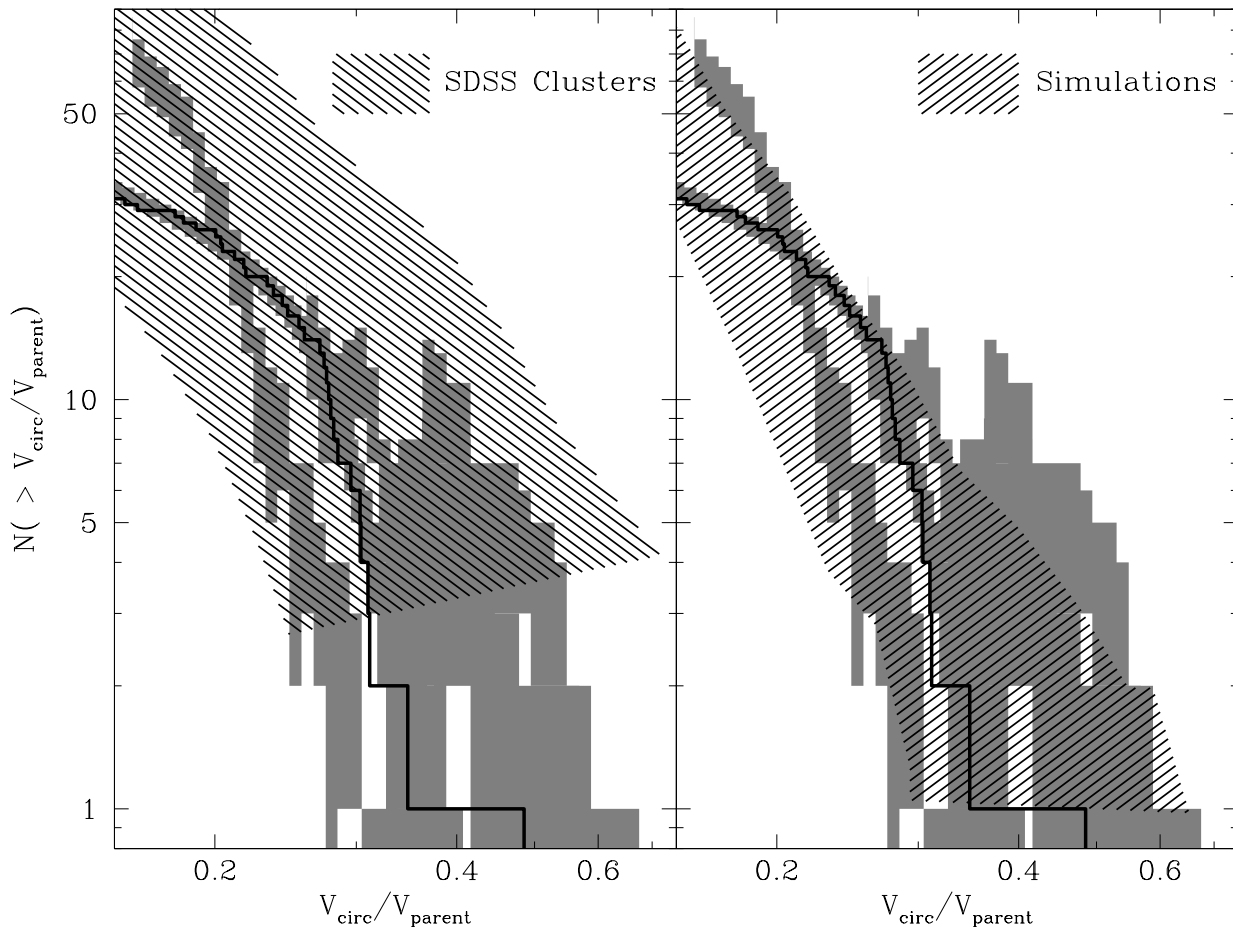


Figure 4. The CSDFs of our five fossil systems (gray shaded areas, displaying the range of statistical uncertainties, same as cyan areas in Fig. 3) compared to CSDFs measured for 34 SDSS clusters of galaxies (hatched area, *left panel*) and simulated clusters (hatched area, *right panel*) from Desai et al. (2004). The CSDF of AWM 4 is highlighted by the thick black line.

sil systems. In other words, the presence of a large magnitude gap between the first and second ranked members of a group/cluster does not imply anything special about its substructure, which can be fully accounted for by existing LCDM simulations.

Interestingly, we also observe a systematic shift of the CSDFs toward lower $V_{\text{circ}}/V_{\text{parent}}$ at increasing V_{parent} . This can be reproduced using the scaling relations of first and second brightest members vs. halo mass derived for a representative sample of groups and clusters by Yang, Mo, & van den Bosch (2008). Once more, this reinforces the idea that fossil systems are not anomalous as far as scaling relations are concerned.

Further deep, wide-field spectroscopic observations of fossil systems are required to confirm the results we have obtained in the present work. This is particularly necessary at the low end of the mass range. On the theoretical side, analyses which mimic observational approaches such as that described here would allow us to compare real data and simulations on an equal footing. This paper is the first in a series which will characterise many of these aspects of fossil groups.

ACKNOWLEDGEMENTS

We thank Simon White and Hans-Walter Rix for useful comments. S.Z. acknowledges the hospitality of the Max-Planck-Institut für extraterrestrische Physik in Garching. D.P. acknowledges useful discussions with E. D’Onghia and the hospitality of the Institute for Theoretical Physics of the University of Zürich. D.P. acknowledges support from the German *Deutsches Zentrum für Luft- und Raumfahrt*, DLR project number 50 OR 0405. G.W.P. acknowledges support from DfG Transregio Programme TR 33.

Funding for the SDSS and SDSS-II has been provided by the Alfred P. Sloan Foundation, the Participating Institutions, the National Science Foundation, the U.S. Department of Energy, the National Aeronautics and Space Administration, the Japanese Monbukagakusho, the Max Planck Society, and the Higher Education Funding Council for England. The SDSS Web Site is <http://www.sdss.org/>. The SDSS is managed by the Astrophysical Research Consortium for the Participating Institutions. The Participating Institutions are the American Museum of Natural History, Astrophysical Institute Potsdam, University of Basel, University of Cambridge, Case Western Reserve Univer-

sity, University of Chicago, Drexel University, Fermilab, the Institute for Advanced Study, the Japan Participation Group, Johns Hopkins University, the Joint Institute for Nuclear Astrophysics, the Kavli Institute for Particle Astrophysics and Cosmology, the Korean Scientist Group, the Chinese Academy of Sciences (LAMOST), Los Alamos National Laboratory, the Max-Planck-Institute for Astronomy (MPIA), the Max-Planck-Institute for Astrophysics (MPA), New Mexico State University, Ohio State University, University of Pittsburgh, University of Portsmouth, Princeton University, the United States Naval Observatory, and the University of Washington.

This research has made use of the NASA/IPAC Extragalactic Database (NED) which is operated by the Jet Propulsion Laboratory, California Institute of Technology, under contract with the National Aeronautics and Space Administration.

REFERENCES

- Adelman-McCarthy J. K., et al., 2008, *ApJS*, 175, 297
- Albert C. E., White R. A., Morgan W. W., 1977, *ApJ*, 211, 309
- Arnaud M., Pointecouteau E., Pratt G. W., 2005, *A&A*, 441, 893
- Baldry I. K., Glazebrook K., Brinkmann J., Ivezić Ž., Lupton R. H., Nichol R. C., Szalay A. S., 2004, *ApJ*, 600, 681
- Barnes J. E., 1989, *Nature*, 338, 123
- Bernardi M., et al., 2003a, *AJ*, 125, 1817
- Bernardi M., et al., 2003b, *AJ*, 125, 1849
- Bernardi M., et al., 2003c, *AJ*, 125, 1866
- Bernardi M., Hyde J. B., Sheth R. K., Miller C. J., Nichol R. C., 2007, *AJ*, 133, 1741
- Bruzual G., Charlot S., 2003, *MNRAS*, 344, 1000
- Csabai I., Budavári T., Connolly A. J., Szalay A. S., Györy Z., Benítez N., Annis J., Brinkmann J., Eisenstein D., Fukugita M., Gunn J., Kent S., Lupton R., Nichol R. C., Stoughton C., 2003, *AJ*, 125, 580
- Cypriano E. S., Mendes de Oliveira C. L., Sodr   L. J., 2006, *AJ*, 132, 514
- De Lucia G., Kauffmann G., Springel V., White S. D. M., Lanzoni B., Stoehr F., Tormen G., Yoshida N., 2004, *MNRAS*, 348, 333
- Desai V., Dalcanton J. J., Mayer L., Reed D., Quinn T., Governato F., 2004, *MNRAS*, 351, 265
- de Vaucouleurs G., de Vaucouleurs A., Corwin, Jr. H. G., Buta R. J., Paturel G., Fouque P., 1991, *Third Reference Catalogue of Bright Galaxies*. Volume 1-3, XII, 2069 pp. 7 figs.. Springer-Verlag Berlin Heidelberg New York
- D’Onghia E., Lake G., 2004, *ApJ*, 612, 628
- D’Onghia E., Sommer-Larsen J., Romeo A. D., Burkert A., Pedersen K., Portinari L., Rasmussen J., 2005, *ApJ*, 630, L109
- Faber S. M., Jackson R. E., 1976, *ApJ*, 204, 668
- Ferrarese L., 2002, *ApJ*, 578, 90
- Gastaldello F., Buote D. A., Humphrey P. J., Zappacosta L., Bullock J. S., Brighenti F., Mathews W. G., 2007, *ApJ*, 669, 158
- Gastaldello F., Buote D. A., Brighenti F., Mathews W. G., 2008, *ApJ*, 673, L17
- Gavazzi G., Zibetti S., Boselli A., Franzetti P., Scodreggio M., Martocchi S., 2001, *A&A*, 372, 29
- Hinshaw G., et al., 2008, *ArXiv e-prints*, 803
- Jansen F., Lumb D., Altieri B., Clavel J., Ehle M., Erd C., Gabriel C., Guainazzi M., Gondoin P., Much R., Munoz R., Santos M., Schartel N., Texier D., Vacanti G., 2001, *A&A*, 365, L1
- Jarrett T. H., Chester T., Cutri R., Schneider S., Skrutskie M., Huchra J. P., 2000, *AJ*, 119, 2498
- Jeltema T. E., Mulchaey J. S., Lubin L. M., Fassnacht C. D., 2007, *ApJ*, 658, 865
- Jones C., Forman W., 1999, *ApJ*, 511, 65
- Jones L. R., Ponman T. J., Forbes D. A., 2000, *MNRAS*, 312, 139
- Jones L. R., Ponman T. J., Horton A., Babul A., Ebeling H., Burke D. J., 2003, *MNRAS*, 343, 627
- J  rgensen I., Franx M., Kjaergaard P., 1995, *MNRAS*, 276, 1341
- Khosroshahi H. G., Maughan B. J., Ponman T. J., Jones L. R., 2006, *MNRAS*, 369, 1211
- Khosroshahi H. G., Ponman T. J., Jones L. R., 2007, *MNRAS*, 377, 595
- Klypin A., Kravtsov A. V., Valenzuela O., Prada F., 1999, *ApJ*, 522, 82
- Koranyi D. M., Geller M. J., 2002, *AJ*, 123, 100
- Lin Y.-T., Mohr J. J., 2004, *ApJ*, 617, 879
- Mendes de Oliveira C. L., Cypriano E. S., Sodr   L. J., 2006, *AJ*, 131, 158
- Milosavljevi   M., Miller C. J., Furlanetto S. R., Cooray A., 2006, *ApJ*, 637, L9
- Morgan W. W., Kayser S., White R. A., 1975, *ApJ*, 199, 545
- Nagai D., Kravtsov A. V., Vikhlinin A., 2008, *ApJ*, 668, 1
- Navarro J. F., Frenk C. S., White S. D. M., 1997, *ApJ*, 490, 493
- O’Sullivan E., Vr  tilek J. M., Kempner J. C., David L. P., Houck J. C., 2005, *MNRAS*, 357, 1134
- Pfeffermann E., Briel U. G., Hippmann H., Kettenring G., Metzner G., Predehl P., Reger G., Stephan K.-H., Zombeck M., Chappell J., Murray S. S., 1987, in Koch E.-E., Schmahl G., eds, *Soft X-ray optics and technology; Proceedings of the Meeting, Berlin, Federal Republic of Germany, Dec. 8-11, 1986*, Bellingham, WA, Society of Photo-Optical Instrumentation Engineers, Volume 733, 1987, p. 519. Vol. 733 of Presented at the Society of Photo-Optical Instrumentation Engineers (SPIE) Conference, The focal plane instrumentation of the ROSAT Telescope. pp 519+–
- Pierini D., 1999, *A&A*, 352, 49
- Pierini D., Gordon K. D., Witt A. N., 2003, *RMxAC*, 17, 200
- Pizagno J., Prada F., Weinberg D. H., Rix H.-W., Pogge R. W., Grebel E. K., Harbeck D., Blanton M., Brinkmann J., Gunn J. E., 2007, *AJ*, 134, 945
- Pizzella A., Corsini E. M., Dalla Bont   E., Sarzi M., Coccato L., Bertola F., 2005, *ApJ*, 631, 785
- Ponman T. J., Bertram D., 1993, *Nature*, 363, 51
- Ponman T. J., Allan D. J., Jones L. R., Merrifield M., McHardy I. M., Lehto H. J., Luppino G. A., 1994, *Nature*, 369, 462
- Popesso P., B  hringer H., Brinkmann J., Voges W., York D. G., 2004, *A&A*, 423, 449

- Popesso P., Böhringer H., Romaniello M., Voges W., 2005, *A&A*, 433, 415
- Sales L. V., Navarro J. F., Lambas D. G., White S. D. M., Croton D. J., 2007, *MNRAS*, 382, 1901
- Salucci P., Lapi A., Tonini C., Gentile G., Yegorova I., Klein U., 2007, *MNRAS*, 378, 41
- Santos W. A., Mendes de Oliveira C., Sodré L. J., 2007, *AJ*, 134, 1551
- Strauss M. A., et al., 2002, *AJ*, 124, 1810
- Sun M., Voit G. M., Donahue M., Jones C., Forman W., 2008, arXiv0805.2320
- Tully R. B., Fisher J. R., 1977, *A&A*, 54, 661
- Tully R. B., Pierce M. J., Huang J.-S., Saunders W., Verheijen M. A. W., Witchalls P. L., 1998, *AJ*, 115, 2264
- Vikhlinin A., McNamara B. R., Hornstrup A., Quintana H., Forman W., Jones C., Way M., 1999, *ApJ*, 520, L1
- Vikhlinin A., Kravtsov A., Forman W., Jones C., Markevitch M., Murray S. S., Van Speybroeck L., 2006, *ApJ*, 640, 691
- Vikhlinin A., Burenin R. A., Ebeling H., Forman W. R., Hornstrup A., Jones C., Kravtsov A. V., Murray S. S., Nagai D., Quintana H., Voevodkin A. 2008, arXiv0805.2207
- von Benda-Beckmann A. M., D’Onghia E., Gottlöber S., Hoeft M., Khalatyan A., Klypin A., Müller V., 2008, *MNRAS*, 386, 2345
- Wegner G., Colless M., Saglia R. P., McMahan R. K., Davies R. L., Burstein D., Baggle G., 1999, *MNRAS*, 305, 259
- Weisskopf M. C., Tananbaum H. D., Van Speybroeck L. P., O’Dell S. L., 2000, in Truemper J. E., Aschenbach B., eds, *Proc. SPIE Vol. 4012*, p. 2-16, X-Ray Optics, Instruments, and Missions III, Joachim E. Truemper; Bernd Aschenbach; Eds. Vol. 4012 of Presented at the Society of Photo-Optical Instrumentation Engineers (SPIE) Conference, Chandra X-ray Observatory (CXO): overview. pp 2-16
- Yang X., Mo H. J., van den Bosch F. C., 2008, *ApJ*, 676, 248
- York D. G., et al., 2000, *AJ*, 120, 1579
- Zibetti S., Gavazzi G., Scodreggio M., Franzetti P., Boselli A., 2002, *ApJ*, 579, 261

APPENDIX A: NOTES ON INDIVIDUAL OBJECTS

A1 AWM 4

AWM 4 belongs to a special subset of poor clusters, originally selected in the optical by Morgan, Kayser & White (1975, MKW) and Albert, White & Morgan (1977, AWM) in a search for cD-like galaxies outside rich clusters, where these galaxies had traditionally been found. NGC 6051, $V_T^0 = 12.93$ mag (de Vaucouleurs et al. 1991), located at $z = 0.031755 \pm 0.000033$ (Wegner et al. 1999), is the cD of AWM 4. Koranyi & Geller (2002) subsequently identified 28 members brighter than $R = 15.5$ mag. Most are early-type galaxies, concentrated in the center and with a smooth Gaussian velocity distribution centered at the velocity of NGC 6051. The velocity dispersion of the system is 440 km s^{-1} .

AWM 4 first appeared as an extended X-ray source in

the catalogue of images of galaxy clusters detected by the *Einstein* Imaging Proportional Counter (Jones & Forman 1999). No substructure nor a departure from symmetry was found in this X-ray image of AWM 4 at a 24 arcsec-resolution. This has been confirmed by the latest X-ray observations, with *XMM-Newton* and at a resolution of 6 arcsec (O’Sullivan et al. 2005), where the X-ray emission is centred on NGC 6051. Despite the presence of a powerful AGN (see Gastaldello et al. 2008, for a thorough discussion), the relaxed appearance of AWM 4 both in optical and X-rays motivated Gastaldello et al. (2007) to include this system in their sample of 16 bright relaxed groups/clusters to which they applied a hydrostatic analysis to measure mass profiles. We use the results of their best fitting NFW profile to characterise the DM halo of AWM 4. The resulting total mass, $1.6 \times 10^{14} M_\odot$, and X-ray temperature, 2.5 keV, qualify AWM 4 as a poor cluster.

Lin & Mohr (2004) first pointed out that AWM 4 appears to be a fossil system, since it is X-ray luminous and meets the magnitude-gap criterion in Ks band⁸. Within a half of the projected virial radius from the X-ray center of AWM two spectroscopic members have the same Ks-band magnitude gap from NGC 6051, of $\Delta m = 2.2$ mag. However, fossil groups were defined using R-band photometry (Jones et al. 2003). In the following we show that the gap is present in R band too. AWM 4 is covered by SDSS imaging and spectroscopy out to its virial radius. Only 4 over 135 spectroscopic targets (see Strauss et al. 2002, for the spectroscopic target selection in the SDSS) do not have a valid redshift measurement down to the limit of $r = 17.77$ mag (corrected for Galactic extinction), corresponding to the absolute magnitude $M_r = -17.91$ mag at the redshift of AWM 4 for the average k -correction. The spectroscopic completeness reaches 100% at $r = 17.25$ mag; it decreases to 90% between 17.25 and 17.77 mag. This allows us to perform a complete cluster-member identification that is almost a factor 10 deeper in luminosity than previously done by Koranyi & Geller (2002). Moreover, the superior photometric quality of the SDSS images allows us to establish the status of AWM 4 as fossil system, by safely assuming that the gap in r band is the same as in R band.

We identify as members all galaxies within the projected virial radius with spectroscopic redshift that differs from the velocity of the system by less than 1000 km s^{-1} . We find a total of 42 members, 23 within half of the virial radius (including NGC 6051). As SDSS photometry is known to underestimate the luminosity of large galaxies (see, e.g., Bernardi et al. 2007) because of the problematic sky subtraction inherent in the automatic pipeline, we perform our own photometric measurements on the original r -band SDSS “corrected frames” for all galaxies within $0.5R_{200}$, following the same procedure described in Gavazzi et al. (2001). The sky background is measured in empty areas, sufficiently far away from galaxies, after masking stars. Elliptical isophotes are fitted to the images of individual galaxies using the IRAF task *ellipse*, after carefully masking contaminating sources, in particular the bright star projected on top of NGC 6051.

⁸ Photometry in the J, H, and Ks bands, complete down to Ks = 13.5, is available from the Two Micron All-Sky Survey extended source catalogue (2MASS, Jarrett et al. 2000).

The resulting 1-D azimuthally-averaged surface brightness profiles are fitted with analytical functions (exponential, de Vaucouleurs or combined). Finally, total magnitudes are derived by extrapolating the measured flux to infinity, according to the best fitting analytic model. As expected, the luminosities of the brightest galaxies are significantly underestimated by the SDSS automatic pipeline. By comparing the so-called ‘model’ magnitudes from the SDSS-DR6 with our own measurements, we find that NGC 6051 is reported 0.67 magnitude too faint, while other galaxies down to ≈ 15 mag are systematically fainter by 0.1 to 0.2 magnitude.

Magnitudes for the three brightest members of AWM 4 are reported in Table A1. All magnitudes are corrected for foreground Galactic extinction. Column 4 lists our extrapolated magnitudes, reported along with the statistical uncertainty due to photometric errors and fitting uncertainties, and upper and lower systematic shifts due to background uncertainties. Column 5 contains our magnitude determinations within the isophotal ellipse corresponding to 25 mag arcsec⁻². Column 6 and 7 are the Petrosian and model magnitudes from the SDSS, respectively.

From our extrapolated magnitudes we conclude that AWM 4 fulfills the requirement of magnitude gap ≥ 2 mag in r band ($\approx R$ band), with a $\Delta m_{12} = 2.23 \pm 0.11^{+0.21}_{-0.27}$ mag. Comparison with the other magnitude determinations and the systematic uncertainty due to the background level also demonstrate how critical the inclusion of the diffuse envelope of the cD is in establishing AWM 4 as a genuine fossil system.

A2 RX J1256.0+2556

RX J1256.0+2556 is one of the fossil groups originally included in the sample of Jones et al. (2003). These authors reported that the presence of the magnitude gap within $0.5R_{\text{vir}}$ critically depends on the exact value of R_{vir} . Although a better determination is now available from Khosroshahi et al. (2007), the uncertainty on the X-ray temperature of this system (2.63 ± 1.13 keV) translates into a large uncertainty on $R_{200} = 1.03^{+0.24}_{-0.28}$ Mpc = $4.66^{+1.08}_{-1.26}$ arcmin. The galaxy [JML2007] J125557.90+255819.6 (whose membership is confirmed by Jeltema et al. 2007) is only 1.2 mag fainter than the brightest member and is located at $1.96'$ from the peak of the X-ray emission. All other potential members with distance $\leq 1.96'$ have a magnitude difference with respect to the cD in excess of 2 mag. The uncertainty on R_{200} therefore does not allow us to establish whether the ≥ 2 mag gap is present or not inside $0.5R_{200}$.

Although Jeltema et al. (2007) have conducted a spectroscopic campaign on RX J1256.0+2556, we can not rely on their data to study the CSDF of this system due to the relatively high incompleteness of their survey (45–90% at $V = 20.5$), and especially the limited span of their data (the inner 700 kpc, thus only 70% of R_{200}). On the other hand, SDSS-DR6 only provides sparse spectroscopic redshifts in this region. Therefore, for the following analysis we will rely on SDSS photometric data alone.

A3 RX J1331.5+1108

This group has the lowest temperature (0.81 keV) in our sample. From available SDSS spectroscopy and photome-

try we find $\Delta m_{12} = 1.93$ mag (SDSS model magnitudes), with the second brightest member within $0.5R_{200}$ (SDSS J133141.49+110644.6) being located at $3.07' = (0.493 \pm 0.013)R_{200}$ from the X-ray peak. As for AWM 4, we perform our own photometric analysis and find a gap $\Delta m_{12} = 2.17$ mag instead. The disagreement with SDSS is possibly generated by sky oversubtraction for the brightest galaxy in the SDSS photometric pipeline. Thus we confirm this group as a genuine fossil.

A4 RX J1340.6+4018

This group is the fossil group archetype (Ponman et al. 1994). The magnitude gap is unambiguous here: the second brightest extended object within $0.5R_{200}$ is ≈ 2.6 mag fainter than the cD. DL04 based their claim for a substructure crisis in fossil groups scale on data from this object. Contrary to DL04, who approximated the circular velocity of this group with $V_{\text{parent}} = \sqrt{\sigma}$ (σ being the 1D projected velocity dispersion of the group reported by Jones et al. 2000), we use more accurate X-ray determinations, but obtain a very similar value, within 30 km s^{-1} .

A5 RX J1416.4+2515

This system, with its $M_{200} \approx 3 \times 10^{14} M_{\odot}$, is rather a poor cluster than a group. It has recently been studied by Cypriano et al. (2006), who obtained spectroscopic redshift and studied the luminosity function in the inner $\approx 3'$ ($\approx 0.35R_{200}$). They confirm a magnitude gap of $\Delta m_{12} = 16.73 - 14.19 = 2.54$ mag in i band (AB), which we can safely assume to be close enough to the gap in R band. Although the region within $0.5R_{200}$ is not completely covered by their survey, we check against SDSS imaging that no brighter member is missed. It is worth noting, once again, that the SDSS magnitude for the cD is severely underestimated by 0.54 i -mag and therefore would not have allowed a reliable estimation of the magnitude gap to be obtained.

The limited coverage provided by the observations in Cypriano et al. (2006) forces us to rely on SDSS photometry to compute the CSDF.

A6 RX J1552.2+2013

Similarly to RX J1416.4+2515, RX J1552.2+2013 is a poor cluster and has been the target of a spectroscopic campaign aimed at determining membership and LF (Mendes de Oliveira et al. 2006). As in the previous case, the coverage is limited to the inner $\approx 3'$ ($\approx 0.4R_{200}$). Mendes de Oliveira et al. (2006) report a gap $\Delta m_{12} \approx 2.2$ mag in i band (AB; see their Fig. 2). However, by inspecting a larger region using SDSS images, at $2.6'$ from the X-ray peak we find an elliptical galaxy (SDSS J155201.61+201350.5) of 16.0 i -mag, that is only 1.2 mag fainter than the brightest cluster galaxy. This galaxy is missing from the sample of Mendes de Oliveira et al. (2006), likely because is only partly included in their image (their Fig. 1). For this galaxy, SDSS gives a photometric redshift of 0.15, hence fully consistent with the redshift of the cluster. Assuming that this redshift is correct and our determination

Table A1. Photometry of the three brightest member galaxies in AWM 4

Rank	RA	Dec	mag_∞	$\text{mag}_{\mu 25}$	Petrosian	model
(1)	(J2000.0) (2)	(J2000.0) (3)	(4)	(5)	(6)	(7)
1 (cD, NGC 6051)	16:04:56.79	+23:55:56.4	$11.92 \pm 0.11^{+0.21}_{-0.27}$	12.46	12.72	12.60
2	16:05:17.61	+23:45:20.4	$14.15 \pm 0.03^{+0.02}_{-0.02}$	14.27	14.44	14.37
3	16:04:50.55	+23:58:29.6	$14.73 \pm 0.03^{+0.02}_{-0.02}$	14.77	14.83	14.70

of R_{200} is correct, even if only within the large uncertainties quoted in Table 2, this cluster does not qualify as fossil.